

Zero-refractoriness spirals in phase-coupled excitable media

E. Ávalos,¹ Pik-Yin Lai,^{1,2,*} and C. K. Chan^{1,2,†}

¹*Department of Physics, Graduate Institute of Biophysics and Center for Complex Systems, National Central University, Chung-Li, 320 Taiwan, Republic of China*

²*Institute of Physics, Academia Sinica, Taipei, 115 Taiwan, Republic of China*

(Received 7 May 2009; published 4 December 2009)

Effects of excitability and coupling strength on plane and spiral waves in two-dimensional excitable lattices modeled by phase-coupled elements are investigated. The corresponding phase diagrams for stable plane waves and spiral waves are obtained by simulations. The parameters capable of supporting stable spiral waves are sorted out together with the spiral rotation frequencies. This discrete model corresponds to an excitable medium with zero refractoriness and in the continuum limit supports zero-core spiral waves. The associated wave propagating behaviors are also discussed analytically and verified.

DOI: 10.1103/PhysRevE.80.065202

PACS number(s): 05.45.Xt, 87.18.Hf, 87.19.Hh

I. INTRODUCTION

Spiral waves in excitable media are robust self-organized patterns ubiquitous in diverse physicochemical and biological systems as in the Beluzov-Zhabotinsky reaction [1], chicken retina [2], social organization of dictyostelium discoideum [3], or in cardiac tissues [4]. Traditionally, the dynamics of the elements in these excitable media capable of supporting spiral waves are modeled by the coupling of a fast (excitatory) and a slow (inhibitory) variables. To distribute the excitatory activity across media, usually diffusive coupling is assumed between these excitable elements. This modeling of excitable media by the interaction of a fast and a slow variable has been very successful. Many observed phenomena associated with spiral waves such as spiral tip meandering [5,6], dependence of wave velocity on wave front curvature, and etc. are correctly reproduced. The famous Oregonator [7], FitzHugh-Nagumo [8], and Luo-Rudy [9] models are entirely based on this scheme. It raises the question whether this slow and fast variable model is the only candidate for the generation of stable spiral waves. It had been shown by Poullet and Ermentrout [10] that stable spiral wave solutions exist for an excitable system which is properly phase coupled. This last finding hints that there are alternatives of generating spiral waves.

Phase models of interacting excitable elements were first attempted by Kuramoto *et al.* [11,12] to describe the ordered phases of ensembles of collection of nonuniform elements. The oscillating limit of this lattice model is well known as the Kuramoto model [13–15]. Recently, collective excitations resulting from ensembles of excitable Kuramoto cells have been considered using globally coupled elements [16,17]. However, properties of spiral waves in phase-coupled model are much less studied and little is known about the stability regime and wave kinematics nor its relation to the continuous reaction-diffusion system is examined. In a fast-slow variables model, the dynamics of the slow variable is needed to reset the fast variable from its excited

state to its rest state during the refractory period of the system. However, in a phase model, the phase variable will automatically reset to zero once it attains the value of 2π because the coupling in the system cannot distinguish the difference between zero and 2π . Therefore, there will be zero refractoriness in a phase-coupled system. Recently, the case of strongly reduced refractoriness in the fast-slow model has also been studied by Zykov [18]. An interesting consequence of zero refractoriness in Zykov's model is that there will be a zero-core spiral in certain limits. From a physical point of view, a zero-refractoriness spiral wave would be more stable since there will be no interaction between the spiral front and the back of the previous spiral wave, thus would not induce instability for meandering.

Furthermore, there are experimental observations of spontaneous wave activities in cultured excitable cardiac ventricle cells [19,20], i.e., the originally excitable (long refractory period) cells become self-oscillatory due to coupling and thus could presumably be modeled by phase-coupled models. In this Rapid Communication, we report the result of our study on dynamics of plane and spiral waves in the Kuramoto excitable model on a lattice of excitable elements phase coupled to its nearest neighbors. The zero-core spiral waves can in fact be reproduced. The properties and stability of plane and spiral waves are investigated systematically, with further exploration on the connections with the continuous reaction-diffusion system.

II. PHASE-COUPLED EXCITABLE MODEL: DISCRETE MODEL AND CONTINUUM LIMIT

We model a large set of coupled excitable elements on a square lattice. Each cell in the lattice is described by the phase ϕ_i that is locally coupled in phase difference to its nearest neighbors described by the Kuramoto-type model,

$$\frac{d\phi_i}{dt} = \omega_i - b \sin \phi_i + k \sum_{\langle i,j \rangle} \sin(\phi_j - \phi_i). \quad (1)$$

The intrinsic dynamics of an isolated element is described by the first two terms: the frequency $\omega_i > 0$ of each cell can in general be nonuniform and the element can be oscillatory or

*pylai@phy.ncu.edu.tw

†ckchan@gate.sinica.edu.tw

excitable depending on the parameter $b \geq 0$. $\langle i, j \rangle$ denotes summation over nearest neighbors. k is the coupling strength between two neighboring cells.

Kuramoto's seminal work [13] showed that weakly coupled oscillators can be described by the simple phase-coupled equations [given by Eq. (1) with $b=0$] in which the dynamics of the limit cycles can all be described by the phase variables ϕ_s . Excitable medium can be described in Eq. (1) with $b \geq \omega_i$. In this regime, the fixed points are relatively close to each other and if the excitation is larger than some threshold, the trajectory triggers into a long excursion eventually ending up at another stable fixed point. Thus the system behaves as an excitable system and if external perturbations are sufficiently large, oscillatory dynamics will result and may propagate to other elements due to coupling. If these oscillatory dynamics can be sustained indefinitely (as in the case of spiral waves), these excitable elements will often undergo oscillations and presumably can be described by a phase-coupled model like that of Eq. (1). Thus we expect coupled excitable elements described by Eq. (1) would be valid for a system whose excitability is near its threshold, which is the regime we will focus here. In coupled systems ($k \neq 0$), signal propagates through the lattice with a speed that increases with the intercell coupling.

The continuum limit of Eq. (1) can be written as a simple reaction-diffusion equation of a single phase variable in space and time. We take all elements having the same ω and for notation simplicity, b and k are all expressed in units of ω (t in unit of $1/\omega$) hereafter. The continuum limit is obtained by taking the lattice spacing, Δx , to be small and one can easily obtain the corresponding reaction-diffusion equation for $\phi(x, y, t)$,

$$\partial_t \phi = 1 - b \sin \phi + D \nabla^2 \phi, \quad (2)$$

where the diffusion constant is given by $D = k(\Delta x)^2$. Thus the discrete model [Eq. (1)] reduces to the continuous reaction-diffusion equation for small Δx or equivalently in the large k limit. Since for excitable systems, $b \geq 1$, the reaction term in Eq. (2) will have two zeros in $0 \leq \phi < 2\pi$. Denoting the first and second zeros by φ_o and $\varphi_o + 2\gamma$, φ_o is given by $b \sin \varphi_o = 1$, and γ can be solve explicitly for $b \geq 1$ to give $\gamma = \sqrt{b^2 - 1}$. For convenience, the phase variable is shifted by defining $\Phi \equiv \phi - \varphi_o$, then the reaction-diffusion equation becomes

$$\partial_t \Phi = F(\Phi) + D \nabla^2 \Phi, \quad F(\Phi) = 1 - b \sin(\Phi + \varphi_o). \quad (3)$$

The reaction function $F(\Phi)$ (shown in Fig. 1) is similar to the cubic nonlinearity function that has been studied in detail in many two-variable reaction diffusion systems such as the FitzHugh-Nagumo model. Contrary to the usual two-variable reaction-diffusion equations which consist of a fast and a slow variables, Eq. (1) corresponds to a reaction-diffusion system with zero refractoriness. This can be seen intuitively from the reaction function $F(\Phi)$ in Fig. 1, once the stable fixed point at the origin is perturbed beyond the unstable point at 2γ , the system almost immediately rushes to the stable point 2π , which is periodically identical to the origin. There is no slow excursion and hence no refractory period in this system. Furthermore, since stable spiral waves occur

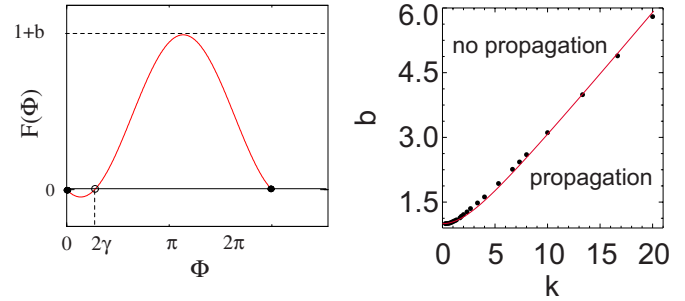


FIG. 1. (Color online) (a) The reaction function $F(\Phi)$ in the continuum limit given by Eq. (3). The stable and unstable fixed points are marked by filled and open circles. (b) Phase diagram for stable plane-wave propagation. The curve is fit of the form $b = \sqrt{1 + \beta k^2}$, where β is a fitting constant.

only in the highly excitable regime in our model and thus the spiral wave produced would approach to a zero-core rigid rotating spiral wave in the large coupling limit.

III. PLANE-WAVE PROPAGATION

The discrete dynamics in Eq. (1) is solved numerically [21]. We study the effect of b and k on the propagation speed for a stable pulse or kink to travel across a section of the lattice. The plane-wave speed v is faster if b is closer to the threshold of excitation. If $b \geq 1$, the distance between the stable and unstable fixed points is short. Hence, the cells on the lattice are highly excitable and thus are able to respond quickly to the front of the excitatory plane wave, allowing a fast signal propagation across the lattice. As shown in the lower inset of Fig. 2, plane wave propagates faster if the value of b is closer to the threshold of excitability. For each value k , it is found that the plane-wave pulse can propagate across the lattice without disruption only if the value of b is sufficiently small. In general the wave speed is larger for stronger coupling, while the wave propagation speed decreases with increasing b . The stability of plane-wave propagation is summarized in the phase diagram in Fig. 1(b), only for systems with strong enough coupling and excitability can support stable plane-wave propagation. The phase boundary

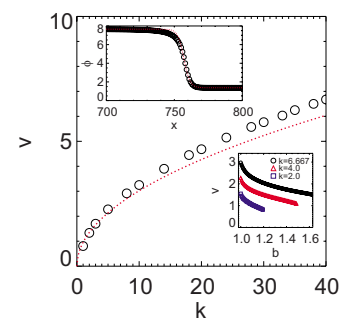


FIG. 2. (Color online) Plane-wave propagation speed as a function of k for $b = 1.02$. The dotted curve is from the theoretical result in Eq. (4). Upper inset: the wave profile of the plane wave for $k = 6$, dotted curve is the theoretical result from Eq. (4). Lower inset: v vs b for different values of k .

can be shown [24] to be of the form $b = \sqrt{1 + \beta k^2}$ (where β is a constant) from nonlinear dynamic analysis.

In the stable regime, an initial arbitrary shape pulse or front of sufficient amplitude will travel and eventually attain a unique stable front with shape and speed determined by b and k . It is worth noting that a similar behavior has been reported in cellular automata model in which plane wave can propagate in excitable medium if the coupling range is sufficiently large [22]. Such a behavior has also been reported in discrete excitable systems [23]. A detail analysis of the corresponding continuum reaction-diffusion model in Eq. (2) also reveals the existence of a minimal k for stable phase kink to propagate [24]. Figure 2 shows the effect of k on the plane-wave speed for a given value of b the propagation velocity increases with k .

For analytic results, we look for traveling wave-front solution of speed v in Eq. (3) of the form $\Phi(x, t) = U(x - vt)$, and the wave-front profile satisfies $DU'' + vU' + F(U) = 0$, with $U(-\infty) = 2\pi$ and $U(\infty) = 0$. One can approximate $F(\Phi)$ by a cubic function with the same maximum and roots as in Fig. 1(a) by $F(\Phi) \approx \mu\Phi(\Phi - 2\gamma)(2\pi - \Phi)$ with $\mu \equiv \frac{27}{16}(1+b)/[\gamma^3 + \pi^3 - \frac{3}{2}\gamma\pi(\gamma + \pi) + (\gamma^2 + \pi^2 - \gamma\pi)^{3/2}]$ and obtain analytically the traveling plane-wave solution. After some algebra, one obtains the plane-wave speed and steady wave-front profile as

$$v = \sqrt{2\mu D}(\pi - 2\gamma), \quad U(z) = \frac{2\pi}{1 + \exp\left[\pi\sqrt{\frac{2\mu}{D}}(z - z_0)\right]}, \quad (4)$$

where z_0 is a constant. The theoretical plane-wave speed is compared with the simulation results of the discrete model in Fig. 2 with no adjustable parameter showing reasonable agreement. The shape of the wave-front profile from the simulation of the discrete model is also compared with the predictions and shown in the upper inset.

IV. SPIRAL WAVES

To induce spiral waves, a propagating plane wave is prepared and then a wave break is set to occur by enforcing half of the cells on a line (perpendicular to propagation direction) to be nonresponsive momentarily. The free shoulder of the broken wave curls and gives rise to a rotating spiral. Figure 3 shows the phase diagram on the stability of spiral waves from Eq. (1) along with the resultant patterns. Systems with large values of k and $b \gtrsim 1$ can support stable spiral waves that persist indefinitely. Stability of spiral waves is further checked by placing an initial regular spiral in lattices with different b and k and observe their evolution dynamics. Snapshots 2 and 4 shows the long time patterns when an initial spiral is placed on the lattice with corresponding values of b and k in the phase diagram. Snapshots 1 and 3 show, respectively, the transient breaking up fragments and the transient unwrapping of the initial spirals, and the system will eventually become quiescent. Regions that do not support stable rotating spiral waves can be described by two regions as labeled by “no sw I” and “no sw II” from their

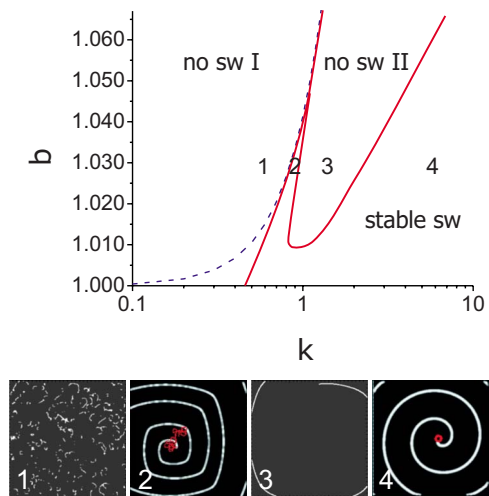


FIG. 3. (Color online) Spiral wave stability phase diagram b vs k on a 300×300 lattice using Eq. (1). Bottom figures shows typical wave patterns and tip trajectories corresponding to the labels indicated on the phase diagram. Note that snapshots 1 and 3 show, respectively, the transient broken fragments and transient unwrapping of initial spirals, while snapshots 2 and 4 show the long time patterns. The dashed curve shows the phase boundary for stable plane-wave propagation [Fig. 1(b)].

different properties. In no sw I, spiral wave is unstable because of the low coupling and there is no stable plane wave in most part of this region. For low excitability (upper part of no sw I), the initial spiral quickly fades away and the medium remains silent; for high excitability (lower part and snapshot 1), the initial SW breaks apart into small pieces of rotating fragments which persist for some time and the medium eventually becomes silent. Stable plane wave can propagate in no sw II, but the coupling is still not strong enough to support a stable spiral wave, an initial spiral will quickly unwrap with long segments exiting from the boundary (snapshot 3). The square-shaped rotating spiral at low coupling (snapshot 2) can be understood to be originated from the discreteness of the model: if the continuum equation in Eq. (2) is discretized with spacing Δx , then a small coupling k corresponds to too coarse a Δx [since $D = k(\Delta x)^2$] which is known to give distorted spirals and hence irregular tip meandering. As k increases near the boundary from region 2 to 3, an initial rotating (round) sw evolves into a squared shaped wave which rotates very slowly. As k increases into region 3, the square spiral stops rotating at all and unfolds into a plane wave, and in region 4 waves propagate as nice rounded spiral waves. The phase boundary for stable plane wave is also shown in the spiral-wave phase diagram. It is clear that region of stable spiral-wave guarantees the stability of plane-wave propagation, but the converse is not true. If k is large enough, the lattice supports rigidly rotating stable spiral waves with the tip tracing out a circle of size of the lattice spacing, i.e., a zero-core spiral wave.

The spiral rotating frequency f as a function of k is shown in the inset of Fig. 4. As is expected, for coupling strength above the stability threshold, the frequency of rotation increases with k and decreases with b . It should be noted that the effect of b on f is several times stronger than due to k . In

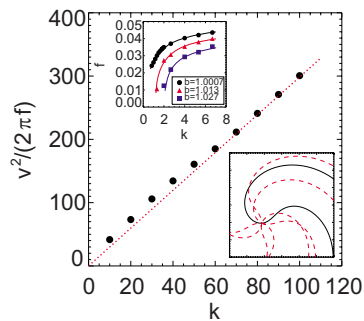


FIG. 4. (Color online) Ratio of the plane-wave propagation speed squared to spiral rotation frequency plotted as a function of coupling strength k . Spiral rotation frequency is measured on a 500×500 lattice with $b=1.02$. The straight line is a fit of the data for larger values of k . Upper inset: rotation frequency of spiral waves vs k for different values of b . Lower inset: snapshots of the rotating spiral wave showing the zero-core behavior for $k=66.67$ and $b=1.007$.

the present case of zero-refractoriness medium, the wave propagation is solely governed by the kinematics of the medium and the spiral rotation angular frequency is related to the plane-wave propagating speed. In the continuum (or large k) limit, the medium will support a zero-core rigidly rotating spiral wave as shown in the lower inset of Fig. 4. In the highly excitable limit (as in this Rapid Communication), spiral rotation frequency is given by [18] $2\pi f=0.331v^2/D$. With the theoretical result in Eq. (4), f is independent of D (or k), the data in the inset of Fig. 4 indeed show that f starts to saturate for large values of k . Furthermore, using $D=k(\Delta x)^2$ in our discrete model, the relation between the spiral-wave rotating frequency and plane-wave speed,

$2\pi f=0.331v^2/D$, can be checked directly. Figure 4 is a plot of v^2/f versus k showing the data fall on a straight line for large k with an inverse slope of 0.335 ± 0.008 which is in excellent agreement with the universal value [18].

From the discussions above, it is clear that our phase-coupled model, in the continuum limit, corresponds to the zero-refractory reaction diffusion system. The associated spiral wave rigidly rotates with a zero core. Contrary to the usual excitable systems with fast and slow variables in which the spiral wave can be depinned and meanders resulting from a Hopf bifurcation [25,26], the single variable phase dynamics in the present model forbids such a mechanism. In experiments, zero-core rigid rotating spiral looks as if the spiral is pinned. Usually, it is assumed that inhomogeneity of the system gives rise to the pinning such as in cardiac cultures [27,28]. Our results suggest that the some apparent pinning of spirals may be naturally arisen from the phase-coupled nature of the excitable medium. In fact, a phase-coupled Kuramoto model [20] has been recently used to understand the phase synchronization in a growing cardiac culture successfully; suggesting that phase coupling is plausible among cardiac cells. Of course, system inhomogeneity would also help pinning spirals in our model.

ACKNOWLEDGMENTS

We thank Professor V. S. Zykov for fruitful discussions and Professor Y. Kuramoto for discussions and for pointing out useful references. This work was supported by the NSC of Taiwan under the Grants No. NSC 98-2112-M008-011-MY3 and No. NSC 96-2112-M001-035-MY3. Support from NCTS of Taiwan is also acknowledged.

- [1] A. T. Winfree, *The Geometry of Biological Time* (Springer-Verlag, New York, 2001).
- [2] M. A. Dahlem and S. C. Müller, *Methods* **21**, 317 (2000).
- [3] G. Gerisch, *Naturwiss.* **58**, 430 (1983); K. J. Lee, E. C. Cox, and R. E. Goldstein, *Phys. Rev. Lett.* **76**, 1174 (1996).
- [4] S. M. Hwang, K. H. Yea, and K. J. Lee, *Phys. Rev. Lett.* **92**, 198103 (2004).
- [5] A. T. Winfree, *Science* **181**, 937 (1973).
- [6] G. Li, Q. Ouyang, V. Petrov, and H. L. Swinney, *Phys. Rev. Lett.* **77**, 2105 (1996).
- [7] P. Gray and S. K. Scott, *Chemical Oscillations and Instabilities: Nonlinear Chemical Kinetics* (Oxford University Press, New York, 1990).
- [8] R. FitzHugh, *Biophys. J.* **1**, 445 (1961); J. Nagumo, S. Arimoto, and S. Yoshizawa, *Proc. IRE* **50**, 2061 (1962).
- [9] C. Luo and Y. Rudy, *Circ. Res.* **68**, 1501 (1991); **74**, 1071 (1994).
- [10] J. E. Paultet and G. B. Ermentrout, *SIAM J. Appl. Math.* **54**, 1720 (1994).
- [11] Y. Kuramoto and T. Yamada, *Prog. Theor. Phys.* **56**, 724 (1976).
- [12] S. Shinomoto and Y. Kuramoto, *Prog. Theor. Phys.* **75**, 1105 (1986); **75**, 1319 (1986); H. Sakaguchi and Y. Kuramoto, *ibid.* **76**, 576 (1986).
- [13] Y. Kuramoto, *Chemical Oscillations, Waves, and Turbulence* (Springer-Verlag, Berlin, 1984).
- [14] J. A. Acebrón, L. L. Bonilla, C. J. Perez, F. Ritot, and R. Spigler, *Rev. Mod. Phys.* **77**, 137 (2005).
- [15] S. H. Strogatz, *Physica D* **143**, 1 (2000).
- [16] C. J. Tessone, A. Scire, R. Toral, and P. Colet, *Phys. Rev. E* **75**, 016203 (2007).
- [17] H. Ohta and S. Sasa, *Phys. Rev. E* **78**, 065101(R) (2008).
- [18] V. S. Zykov, *Phys. Rev. E* **75**, 046203 (2007); *Physica D* **238**, 931 (2009).
- [19] S. J. Woo *et al.*, *New J. Phys.* **10**, 015005 (2008).
- [20] W. Chen *et al.*, *EPL* **86**, 18001 (2009).
- [21] The coupled system of equations are solved by Euler algorithm on square lattices up to sizes 500×500 with open boundary conditions with a time step of 10^{-4} .
- [22] G. Bub, A. Shrier, and L. Glass, *Phys. Rev. Lett.* **88**, 058101 (2002).
- [23] J. P. Keener, *SIAM J. Appl. Math.* **47**, 556 (1987).
- [24] E. Avalos, P. Y. Lai, and C. K. Chan (unpublished).
- [25] A. Karma, *Phys. Rev. Lett.* **65**, 2824 (1990).
- [26] D. Barkley, *Phys. Rev. Lett.* **72**, 164 (1994).
- [27] K. Agladze *et al.*, *Am. J. Physiol. Heart Circ. Physiol.* **293**, H503 (2007).
- [28] A. Isomura, M. Horning, K. Agladze, and K. Yoshikawa, *Phys. Rev. E* **78**, 066216 (2008).